https://doi.org/10.5194/amt-2023-258
Preprint. Discussion started: 5 February 2024


Atmospheric Measurement Techniques Discussions

# Applicability of the inverse dispersion method to measure emissions from animal housings

Marcel Bühler[1,2], Christoph Häni[1], Albrecht Neftel[3], Patrice Bühler[1], Christof Ammann[4], Thomas Kupper[1]

[1]School of Agricultural, Forest and Food Sciences HAFL, Bern University of Applied Sciences, Zollikofen, 3052, Switzerland
[2]Department of Biological and Chemical Engineering, Aarhus University, Aarhus, 8000, Denmark
[3]Neftel Research Expertise, Wohlen bei Bern, 3033, Switzerland
[4]Climate and Agriculture Group, Agroscope, Zürich, 8046, Switzerland

*Correspondence to*: Marcel Bühler (mb@bce.au.dk)

**Abstract.** Emissions from agricultural sources substantially contribute to global warming. The inverse dispersion method has been successfully used for emission measurement from various agricultural sources. The method has also been validated in multiple studies with artificial gas releases mostly on open fields. Release experiments from buildings have been very rare and were partly affected by additional nearby sources of the same gas. What is also lacking are specific release studies for naturally ventilated animal housings. In this study, a known and predefined amount of methane was released from an artificial source inside a barn that mimics a naturally ventilated dairy housing. For concentration measurements, open-path devices (OP) with a path length of 110 m were placed in downwind direction of the barn at a distance of 50 m, 100 m, 150 m, and 200 m and additionally, a 3D ultrasonic anemometer (UA) was placed in the middle of the OP paths at 50 m, 100 m and 150 m. Upwind of the barn, an additional OP and an UA were installed. The median recovery rates of the experiment depending on the used OP and UA combination ranged between 0.56 - 0.71. It is concluded that for the present study case, the effect of the building and a tree in the main wind axis led to a systematic underestimation of the inverse dispersion method derived emission rate probably due to deviations of the wind field and turbulent dispersion from the ideal assumptions.

## 1 Introduction

Methane ($CH_4$) is the second most important greenhouse gas after carbon dioxide. In the last decade, atmospheric $CH_4$ concentrations were dominated by emissions from fossil fuels, agriculture, landfills, and the waste management sector (Stocker et al., 2013). Within the livestock sector at a global scale, $CH_4$ mainly originates from enteric fermentation in the digestive tract of ruminants and to a minor extent from emissions from manure management (Gerber, 2013). A common housing system for cattle is loose housing in naturally ventilated buildings (Sommer et al., 2013). To improve national emission inventories and test mitigation effects under real world conditions, accurate measurements are necessary. For confined sources of greater complexity, the inverse dispersion method (IDM) has been established in the recent years. The IDM is a micrometeorological method that combines concentration measurements up- and downwind of the spatially defined source with an atmospheric

https://doi.org/10.5194/amt-2023-258
Preprint. Discussion started: 5 February 2024


Atmospheric Measurement Techniques Discussions

dispersion model. For agricultural emissions, most often a backward Lagrangian stochastic (bLS) model is used. The IDM with a bLS model has been verified in multiple release experiments on open fields that reflect ideal conditions in terms of Monin-Obukhov-Similarity theory (Flesch et al., 2004). Also, under less ideal conditions in terms of Monin-Obukhov-Similarity theory, the IDM showed its aptitude for a wide range of sources (e.g., Bühler et al., 2022; Bühler et al., 2021; Flesch et al., 2009; Flesch et al., 2013; Laubach et al., 2013; VanderZaag et al., 2008). However, there are only few studies available, where the gas was released within or close to a building structure. Baldé et al. (2016a,b) and Hrad et al. (2021) released $CH_4$ at real-world facilities in addition to the $CH_4$ from sources existing at the sites. McGinn et al. (2006) conducted a release experiment at a barn with three release positions on top of the roof and three positions outside the walls of the barn. Gao et al. (2010) released $CH_4$ via four side vents of a barn. The barn in the study of Gao et al. (2010) is comparable to a mechanically ventilated building which is common for fattening pigs or poultry.

In this paper, we present an experiment with artificial release of $CH_4$ within a building similar to a naturally ventilated dairy housing. The goal of this experiment was to test the IDM for emission measurements from an agricultural building with natural ventilation under as realistic conditions as possible to optimise the quality of the measurement results and minimise the uncertainty range of the IDM. Compared to Gao et al. (2010), multiple 3D ultrasonic anemometers were available in our experiment. Thus, the focus was on the positioning of the open-path concentration sensors and the ultrasonic anemometers at different horizontal distances downwind of the source.

## 2 Material and Methodology

### 2.1 Experimental site and periods

The release experiment was conducted in a barn located in the Central Plateau of Switzerland (47.04307 N, 7.22691 E). The barn allowed a setup which mimicked a naturally ventilated dairy housing. About 350 m northeast of the barn is a river with dams on each side that are 4 m higher than the agricultural land surrounding the barn. The canopy height directly around the barn was 20 cm or lower and remained constant over the course of the measurements. The barn is 25 m long, 17 m wide and 7 m high (Fig. 1). During the release experiment, about 17% of the barn's surface was occupied by storage boxes stacking up almost to the ceiling. Despite other agricultural equipment inside the barn, about 33% of the south end of the barn were empty. The barn had on each transverse side a 4.8 m wide and 4.0 m high gate. During the $CH_4$ releases, the gate on the south side was fully open, whereas the gate on the north side was opened 1.3 m. The north facing wall of the barn was impermeable, however the south wall and the longitudinal side walls exhibited small holes and cracks all over the wall allowing for air exchange through the wall. At both longitudinal sides of the barn there were gaps of about 0.6 m below the roof which were covered by cracked plastic sheets. About 20 m southwest of the barn was a tree of about 15 m height (Fig. 1).

https://doi.org/10.5194/amt-2023-258
Preprint. Discussion started: 5 February 2024


Atmospheric Measurement Techniques Discussions

**Fig. 1. Barn used for the $CH_4$ release experiment. The photo was taken from the southwest side of the barn. In the foreground is a 3D ultrasonic anemometer (UA-50m).**

A petrol-powered generator (Honda EU 20i), located outside the barn at the southeast side, provided the necessary power for all the instruments.

The wind and concentration measurements lasted over several weeks from 05 March to 26 March 2021. A first intercomparison (IC1) of the open-path devices was conducted from 05 March to 10 March 2021. The measurement campaign (MC) took place from 18 March 2021 11:00 to 21 March 2021 13:00 UTC+1. Within this MC, $CH_4$ was released with a $CH_4$ source inside the barn from 19 March 2021 10:30 to 19 March 2021 16:40 UTC+1 and 19 March 2021 21:50 to 20 March 2021 06:50 UTC+1. The second intercomparison (IC2) of the open-path devices was conducted from 21 March 2021 15:00 to 26 March 2021 10:00 UTC+1. $CH_4$ was also released during part of IC2.

### 2.2 Methane source

For the release during MC and half of IC2, a gas bundle of 12 cylinders with 50 L at 200 bars, each with high-purity (> 99.5% mol) $CH_4$, was used to supply the $CH_4$ source. For the rest of the release in IC2, one gas cylinder with 50 L at 200 bars was used. Attached to the bundle was a pressure regulator (Fig. 2). The pressure on the high-pressure side was measured with a digital pressure sensor (LEX1-Ei / 200bar / 81770.5, Keller AG, Winterthur, Switzerland). The low-pressure side was set to 3 bars. The pressure regulator and the mass flow controller (MFC, EL-FLOW Select F-202AV-M20-AGD-22-V, Bronkhorst High-Tech B.V., Ruurlo, The Netherlands) were connected by a polyethylene naphthalate (PEN) tubing (FESTO, PEN-16X2,5-BL-100 551449) with an inner diameter of 10.8 mm. After the MFC, there was an 8 m long PNE tube with an inner

https://doi.org/10.5194/amt-2023-258
Preprint. Discussion started: 5 February 2024


Atmospheric Measurement Techniques Discussions

diameter of 10.8 mm to a gas distribution block made of aluminium with three outlets (ITV, 124 A24 G1/2"). Each outlet had an L-fitting (FESTO, QSL-G1/2-16 186126) and 1.5 m of the same tubing connected to another gas distribution block with eight outlets with a reduction of the tubing diameter to 2.7 mm (FESTO, FR-8-1/4 2078). To each of these outlets a L-fitting (FESTO, QSLL-1/4-4 190662) and a 20 m long with an inner diameter of 2.7 mm PEN tubing (FESTO, PPEN-4X0,75-BL-500 551444) was attached that released the $CH_4$. At the end of these tubes, no pressure reduction was added. The total pressure drop of the system was expected to be around 0.4 bar.

The pressure and the temperature recorded with the Keller pressure sensor were logged with 10 Hz. From the MFC, the setpoint ($L_n$ $min^{-1}$), the flow rate ($L_n$ $min^{-1}$) and the temperature were logged with 0.1 Hz resolution. The MFC had a maximum flow of 160 $L_n$ $min^{-1}$ and was calibrated for $CH_4$ at 15 °C. During IC2, the setpoint was varied between 50 and 160 $L_n$ $min^{-1}$, whereas the flow was kept constant at 140 $L_n$ $min^{-1}$ during the MC. 140 $L_n$ $min^{-1}$ correspond to 6.02 kg $CH_4$ $h^{-1}$ which represents an emission rate of about 360 dairy cows. Under Swiss regulations, the space in the barn would be insufficient for 360 dairy cows, but this emission rate was chosen to achieve sufficient concentration enhancement at the concentration measurement locations and thus an adequate signal to noise ratio. The cumulative flow through the MFC whilst the gas bundle was connected, was within 1% of the $CH_4$ volume inside the gas bundle.

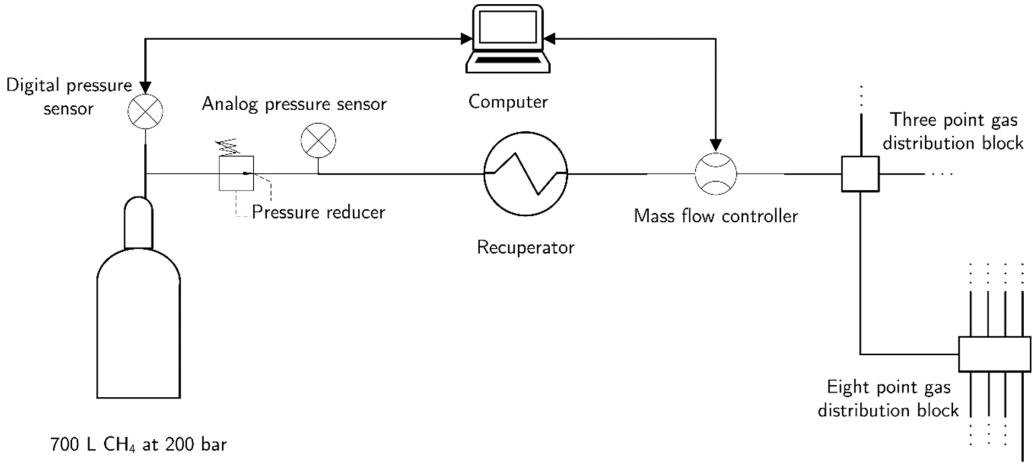


**Fig. 2. Schematic of the $CH_4$ source for the artificial release experiment.**

The gas bundle and the MFC were placed outside the barn on the north side. The release points inside the barn were at 1.5 m above ground. The 24 release points were equally distributed in the southern half of the barn.

In the beginning of the release in the MC, a short circuit caused a shutdown of the power generator for about 30 min. On 20 March 2021 around 01:00 UTC+1, the computer was needed to check data from an UA and thus, the $CH_4$ release was stopped for a few minutes.

https://doi.org/10.5194/amt-2023-258
Preprint. Discussion started: 5 February 2024


Atmospheric Measurement Techniques Discussions

### 2.3 Methane concentration measurements

The $CH_4$ concentrations were measured with five GasFinder3-OP (Boreal Laser Inc., Edmonton, Canada) open-path tunable diode laser absorption spectrometers (hereafter denoted as OP). Twelve-corner cubes mirrors were used as retroreflectors. Data with an insufficient light intensity were removed. Device specific relationships determined by factory calibration were applied to the measured concentration using local air temperature and air pressure measured by a weather station (Lufft WS700-UMB Smart Weather Sensor, G. Lufft Mess- und Regeltechnik GmbH Fellbach, Germany) placed about 100 m southwest from the barn. The measured $CH_4$ concentrations (0.3 – 1 Hz resolution) were averaged to 10 min periods and periods with a data coverage lower than 75% (7.5 min) were removed. The concentrations between the five OP were inter-calibrated with data from the parallel measurements in IC1 and IC2 using linear regression.

### 2.4 Turbulence measurements and data filtering

Four 3D ultrasonic anemometers (UA, Gill Windmaster, Gill Instrument Ltd., Lymington, UK) were used to determine turbulence parameters. A two-axis coordinate rotation was applied for the wind vector rotation. The 10 Hz data were averaged to 10 min periods.

As the dispersion model of the IDM uses Monin-Obukhov similarity theory (MOST) scaling, the UA data required compatibility with MOST assumptions and consequently a screening of data with the goal to exclude situations that substantially deviated from MOST conditions. The goal of this screening or quality filtering was to retain as much data as possible without introducing too many erroneous results. Quality filters were applied for the wind direction and the friction velocity $u_*$. Data with $u_* \leq 0.15$ m s$^{-1}$ were excluded (Flesch et al., 2005). No other quality filters were applied.

### 2.5 Experimental setup

For all measurements, the five OP (sensor modules and retroreflectors) were placed 1.60 m above ground level with a path length of 110 m. In IC1, the OP were placed about 100 m southwest of the barn. During the MC, four OP were placed southwest of the barn and one northeast of the barn (Fig. 3). The absolute distance and the corresponding distance as a multiple of the barn height - denoted here as fetch and given in parentheses - between the barn and the middle of the OP path on the southwest side were 50 m (7.1), 100 m (14.3), 150 m (21.4) and 200 m (28.6). Three UA were placed downwind in the middle of the OP paths and one upwind of the barn. The measuring heights of all UA was at 2.16 m above ground level. For IC2, all five OP were placed next to each other about 50 m southwest of the barn and one UA was placed 55 m southwest from the barn at 2 m above ground level (Fig. S1, supporting information).

https://doi.org/10.5194/amt-2023-258
Preprint. Discussion started: 5 February 2024


Atmospheric Measurement Techniques Discussions

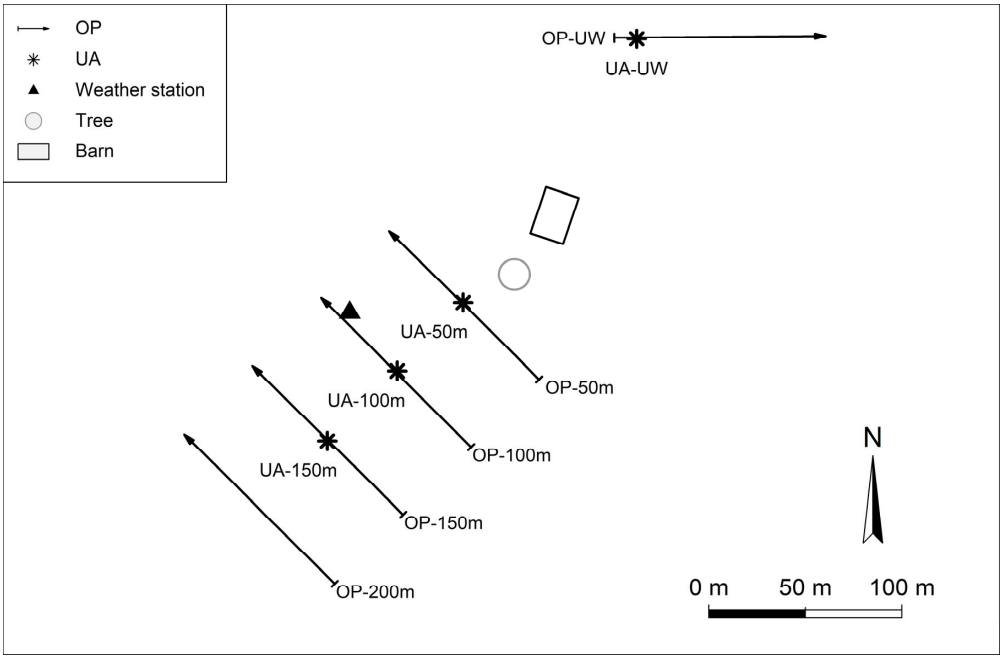


**Fig. 3. Schematic overview of the measurement setup during the measurement campaign. OP = open-path device, UA = 3D ultrasonic anemometer, UW = upwind. The numbers behind the OP and UA represent the meters downwind of the barn. The distances as a multiple of the barn height (fetch) are 7.1 for 50 m, 14.3 for 100 m, 21.4 for 150 m and 28.6 for 200 m.**

### 2.6 Inverse dispersion method

The IDM is a micrometeorological approach to measure emissions from a spatially confined source. It uses an atmospheric dispersion model to establish the relationship between the emission of the source and the concentration measured downwind of the source under investigation. This concentration-emission relationship is quantified by the dispersion factor $D$ (s m$^{-1}$) which depends on the geometrical configuration of source and concentration sensor as well as on the turbulence and the wind field. To separate the contribution of the source from the incoming (background) concentration at the downwind measurement location, the concentration upwind of the source is equally measured. With the area $A$ (m$^{-2}$) of the source the emission of the source $Q$ (kg s$^{-1}$), can be calculated Eq. (1):

$$Q = \frac{C_{DW} - C_{UW}}{D} \cdot A \quad (1)$$

where $C_{UW}$ and $C_{DW}$ are the upwind (background) and downwind concentration (kg m$^{-3}$).

A backward Lagrangian stochastic (bLS) model was used as atmospheric dispersion model (Flesch et al., 1995; Flesch et al., 2004). The bLS model by Flesch et al. (1995) uses MOST formulas to specify turbulence statistics in the inertial sublayer of the atmosphere, that are derived from the friction velocity, the Obukhov length and the roughness length measured by the UA. MOST needs stationarity and homogeneity regarding the turbulence conditions, therefore, the measurement site should be

https://doi.org/10.5194/amt-2023-258
Preprint. Discussion started: 5 February 2024


Atmospheric Measurement Techniques Discussions

horizontal homogeneous and flat over a large area. Additionally, the bLS model assumes a homogeneous diffusive ground source. A building or a structure violates these conditions and thus based on experimental field trials, it is recommended, that the distance between the source and the downwind measurement locations should be not less than 10 times the source height so that the turbulence fulfils the assumptions of homogeneity and stationarity (Gao et al., 2010; Harper et al., 2011).

The OP in the bLS model were approximated by a series of point sensors with a 1-m spacing along the path length. For each of these point sensors and each emission interval, one million backward trajectories were used to calculate the value of $D$. The simulations were run in R Statistical Software (v3.6.6: R Core Team 2019) using the package bLSmodelR (Häni et al., 2018), available at https://github.com/ChHaeni/bLSmodelR.

## 3 Results

A general overview of the weather conditions during the measurement campaign is given in Fig. 4. Due to a change in wind direction, the release was stopped for several hours until the conditions were suitable again. During the first part of the release the inverse Monin-Obukhov length ($1/L$) recorded by UA-UW was between 0 and -0.1 $m^{-1}$, thus the atmospheric conditions were moderately unstable. In the second part of the release, which was mainly during the night, the atmospheric conditions were moderately stable with $1/L$ between 0 and +0.1 $m^{-1}$ (Fig. S2, supporting information).

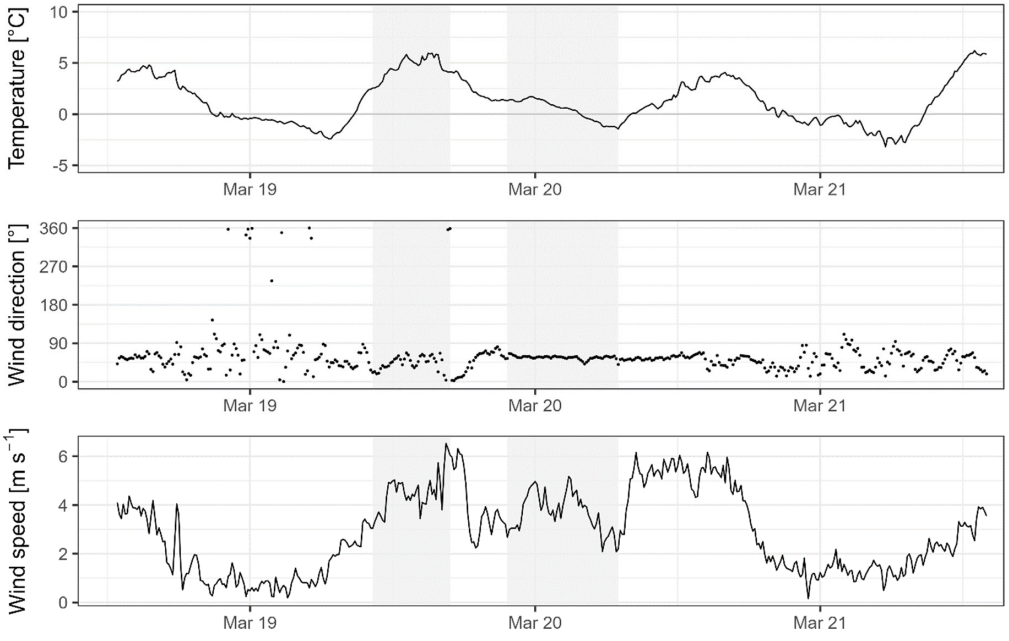


**Fig. 4 Weather conditions measured with the onsite weather station during the measurement campaign. The grey shaded areas indicate the times during which $CH_4$ was released.**

https://doi.org/10.5194/amt-2023-258
Preprint. Discussion started: 5 February 2024


Atmospheric Measurement Techniques Discussions

### 3.1 Influence of the barn on the wind field

The wind direction of the downwind UA deviated between 40° and 65° from the UA-UW with a maximum at around 55° (Fig. 5). The barn was located at 45° of the downwind UA and 225° of the UA-UW, respectively. The closer the downwind UA was placed to the barn, the further the local wind direction deviated towards north from the upwind wind direction measured by UA-UW (Table 1).

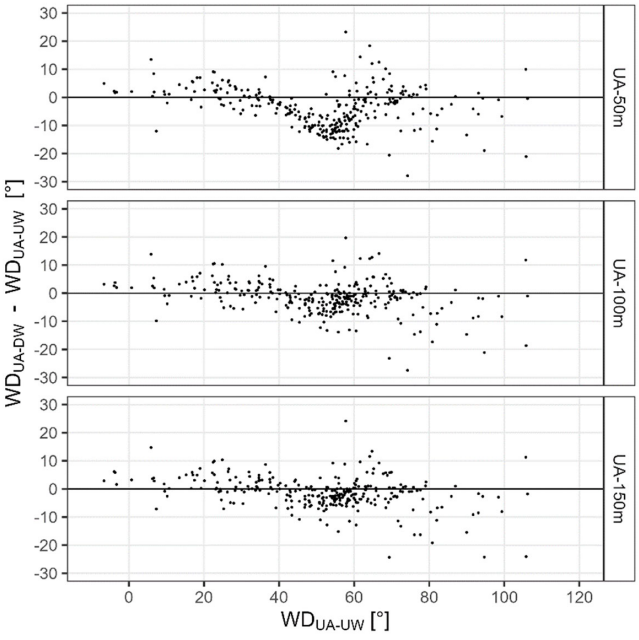


**Fig. 5 Absolute difference in the wind direction between the three downwind UA (UA-DW) and the upwind UA (UA-UW) recorded during the measurement campaign given as 10-min data. The exact locations of the UA are given in Fig. 3.**

The wind speed of the UA closest to the barn was, depending on the wind direction, either higher or lower than the wind speed measured with the UA-UW (Fig. S3, supporting information). At 150 m from the barn, the wind speed was on average 7% higher than at the upwind location. A similar pattern can be seen for the $u_*$ values. For the standard deviation of the $v$ wind divided by friction velocity, the deviations between the UA-UW and the downwind UA are strongest for the 50 m location. For UA-100m and UA-150m there is a constant offset of -0.49 (Fig. S4, supporting information).

https://doi.org/10.5194/amt-2023-258
Preprint. Discussion started: 5 February 2024


Atmospheric Measurement Techniques Discussions

Table 1: Mean wind direction (WD), mean wind speed (WS) and friction velocity ($\boldsymbol{u}_*$) recorded of the four UA during the measurement campaign and while $CH_4$ was released in the measurement campaign.

| | During measurement campaign | | | During $CH_4$ release | | |
|---|---|---|---|---|---|---|
| | Mean WD [°] | Mean WS [m $s^{-1}$] | Mean $u_*$ [m $s^{-1}$] | Mean WD [°] | Mean WS [m $s^{-1}$] | Mean $u_*$ [m $s^{-1}$] |
| UA-UW | 51.6 | 2.6 | 0.19 | 51.6 | 3.5 | 0.28 |
| UA-50m | 46.7 | 2.9 | 0.23 | 45.8 | 3.2 | 0.25 |
| UA-100m | 50.4 | 2.7 | 0.22 | 50.7 | 3.6 | 0.32 |
| UA-150m | 50.8 | 2.9 | 0.23 | 50.7 | 3.8 | 0.32 |

### 3.2 Recovery rates

During the MC whilst $CH_4$ was being released, the data loss due to quality filtering was highest with the combination UA-50m and OP-200m (40%) and lowest with UA-100m and OP-50m (5%). On average, UA-100m, UA-150m and UA-UW showed similar data loss, whereas the data loss for UA-50m was a bit higher (Table 2). The recovery rates (determined emission divided by actual emission) determined from the different UA and OP combinations were on average always below 1 and did not substantially differ during the MC (Table 3, Fig. 6). The median recovery rates ranged between 0.56 - 0.71. The median recovery rate slightly increases with the distance from the OP to the barn for all UA, except for UA-50m.

Table 2 Percentage of data loss of the different UA and OP combinations after quality filtering during the MC whilst being gas was released.

| | UA-UW | UA-50m | UA-100m | UA-150m |
|---|---|---|---|---|
| OP-50m | 8% | 16% | 5% | 6% |
| OP-100m | 11% | 21% | 9% | 11% |
| OP-150m | 29% | 32% | 24% | 22% |
| OP-200m | 36% | 40% | 32% | 31% |
| Average | 21% | 27% | 18% | 18% |

https://doi.org/10.5194/amt-2023-258
Preprint. Discussion started: 5 February 2024


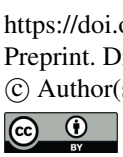

Atmospheric Measurement Techniques Discussions

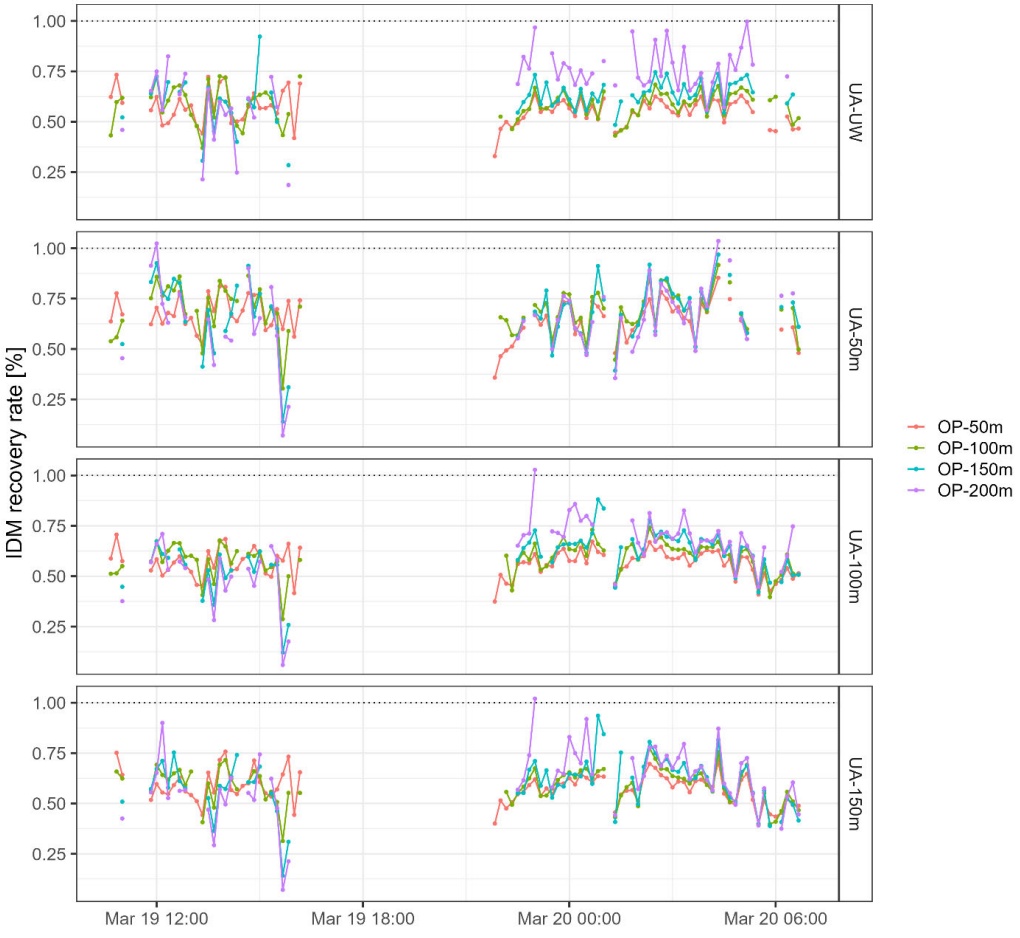


**Fig. 6 Recovery rate for the measurement campaign with all possible UA and OP combinations. Each panel represents an UA and the colours indicates the OP used to calculate the recovery rate. The time series is in UTC+1.**

Table 3: Median recovery rates for all possible OP-UA combinations for the MC whilst being $CH_4$ released.

| | UA-UW | UA-50m | UA-100m | UA-150m | All UA |
|---|---|---|---|---|---|
| OP-50m | 0.56 | 0.65 | 0.58 | 0.58 | 0.59 |
| OP-100m | 0.59 | 0.70 | 0.60 | 0.60 | 0.62 |
| OP-150m | 0.63 | 0.69 | 0.62 | 0.61 | 0.63 |

https://doi.org/10.5194/amt-2023-258
Preprint. Discussion started: 5 February 2024


Atmospheric Measurement Techniques Discussions

| | | | | | |
|---|---|---|---|---|---|
| OP-200m | 0.71 | 0.65 | 0.66 | 0.62 | 0.66 |
| All OP | 0.60 | 0.67 | 0.60 | 0.60 | |

### 3.3 Plume modelling and wind field rotation

With the bLS model it is also possible to model an emission plume by calculating the dispersion factor *D* for every point of a grid laid over the experimental site. For each of the grid points, the expected concentration with the given emission of 6.02 kg $CH_4$ $h^{-1}$, is calculated which allows to establish a contour plot (Fig. 7). For all UA most of the modelled emission plume is within the measurement path of the OP. For UA-UW, UA-100m and UA-150m, the average plume is slightly shifted towards the northwest end of the OP path.

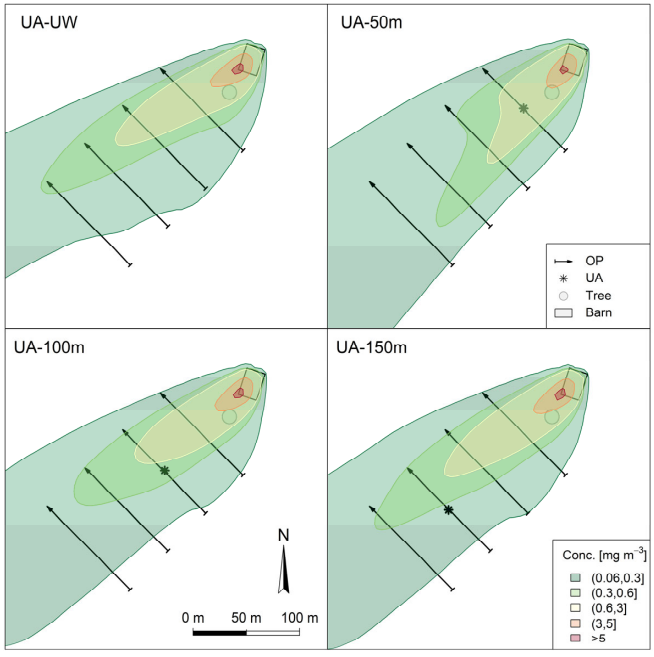


**Fig. 7 Contours of the averages overall modelled emission plumes given as concentration enhancements for the xy-plane at a height of 1.60 m above ground for the bLS runs based on the four UA. The name of the OP and the position of the UA-UW are given in Fig. 3.**

Next to that visualisation, also implications on the recovery rates by rotating the wind field by 10° clock- and anticlockwise in 1°-steps were tested (Fig. 8). The emissions of the OP closest to the barn was almost unaffected by any change in wind direction. The more the OP was placed away from the barn, the larger were the changes in emissions due to the wind field

https://doi.org/10.5194/amt-2023-258
Preprint. Discussion started: 5 February 2024


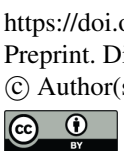

Atmospheric Measurement Techniques Discussions

rotation. Generally, a clockwise shift of the wind field led to higher emissions and an anticlockwise shift led unchanged or lower emission estimates, whereas the changes were more pronounced with a clockwise rotation.

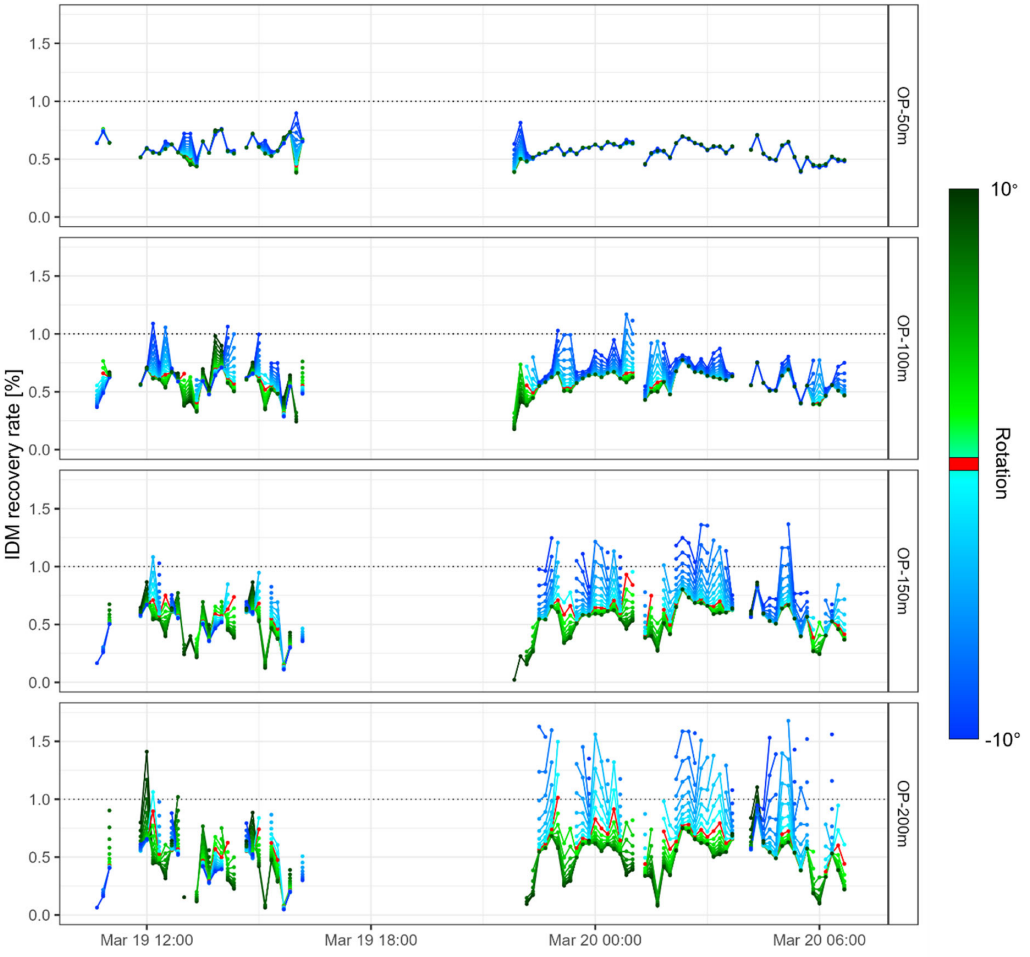


210 **Fig. 8 Effects of the wind field rotation on the IDM recovery rate calculated with UA-150m and the four downwind OP. Each colour represents a rotation by 1°. Green: anticlockwise rotation of the wind field. Blue: clockwise rotation of the wind field. Red: original line. The time series is in UTC+1. Note that due to wind direction filtering (for every run the same) not every run has the same number of data points.**

https://doi.org/10.5194/amt-2023-258
Preprint. Discussion started: 5 February 2024


Atmospheric Measurement Techniques Discussions

## 4 Discussion

### 4.1 Influence of the barn on the wind field

The influence of the barn and the tree on the downwind turbulence measurements is clearly visible. The closer the UA was placed to the barn, the larger was the influence. The wind must flow around the barn and thus the largest deviation in the wind direction was measured at around 55°, which corresponds to the southwest-northeast diagonal of the barn. The wind field deviation is also visible in all other turbulence parameters (Fig. S4, supporting information). Even though some of the devices were placed at a downwind distance of more than the recommended 10 times the barn height away (Harper et al., 2011, Gao et al., 2010), a deviation of the wind direction of the downwind UA compared to the UA-UW due to the barn was still visible at 100 m (fetch = 14.3 times barn height) and 150 m (fetch = 21.4). However, if the 15 m high tree is considered as relevant flow disturbance, the fetch values become considerable smaller, namely 2.0, 5.3, 8.6 and 12.0 for the instrument locations at 50 m, 100 m, 150 m and 200 m, respectively (see Fig. 3).

The difference in the turbulence parameters indicate that the UA were still in the wake of the barn and the tree. This wind field deviation will most likely deviate from the dispersion calculated from the bLS model, but unfortunately, we cannot model that. Consequently, the calculated recovery rates will have a deviation from the expected values.

### 4.2 Quality filtering and data loss

In this measurement campaign, a minimum of quality filters was applied. Compared to other measurement campaigns conducted in Switzerland (Bühler et al., 2022; Bühler et al., 2021), this measurement campaign was of shorter duration and the atmospheric conditions varied less. Additional filters, other than filtering for $u_*$ and the wind direction, were tested but not applied in the final analysis, since they excluded more data but did not alter the findings and the mean and median recovery rates.

### 4.3 Recovery rates

The recovery rates for the UA, except UA-50m, slightly increased with the distances of the OP to the barn. On the other hand, there is no pattern in the recovery rate in terms of increasing distance of the UA from the barn (Fig. S5, supporting information). The recovery rates of the OP closest to the barn are consistent with the findings of Gao et al. (2010), who conducted a similar experiment and achieved a recovery rate of 0.66 for a similar fetch. However, for a fetch of 10 to 25 times the building height, Gao et al. (2010) measured recovery rates between 0.93 and 1.03 while in the present study the median recovery rate for similar fetches (considering the barn as highest point) remained between 0.59 and 0.71.

A bias in the results due to biases in the intercalibration of the OP or in the amount of released gas could be excluded. When the barn was excessively vented after the $CH_4$ release, no increase in the downwind $CH_4$ concentration could be observed, indicating that no $CH_4$ was kept back inside the barn.

https://doi.org/10.5194/amt-2023-258
Preprint. Discussion started: 5 February 2024


Atmospheric Measurement Techniques Discussions

Even though the wind direction deviated by 7° from the expected wind direction, most of the averaged modelled emission plume was still within the open path measurements (Fig. 7). However, the results from the wind field rotation indicate that the modelled emission plume was rather on the edge of the OP measurement paths. Nevertheless, those modulations cannot explain the low recovery rate. There are multiple time intervals where the rotation of the wind field had no effect on the recovery rate and that recovery rate remained distinctly below 1, indicating that an offset in the model wind direction cannot be the sole reason.

Despite having the experiment carefully conducted and long measurement paths, long fetches, high release rates were used, and the terrain was relatively horizontal, homogeneous and flat, the recovery rates were lower than expected. The low recovery rates indicate that the mixing of the released $CH_4$ into the atmosphere was larger than in the bLS model world. This larger mixing could have been in any of the three dimensions. As lateral and vertical mixing are coupled and any changes in one direction has consequences in the two others, disentangling is difficult.

Nevertheless, a possible explanation for the lower recovery rates is that the initial vertical mixing of the $CH_4$ was larger than in the bLS model. Such a larger mixing can occur, because the bLS model assumes a diffusive ground source which releases gas into an ideal flow field. In our case, the gas was actively released inside the barn about 1.5 m above ground and might have left the barn at an even higher height above ground. More importantly, the wake caused by the barn and its interaction with the tree could have led to a strong updraft and consequently increased vertical mixing.

To verify this hypothesis, a vertical profile of the $CH_4$ concentrations at the same OP locations would have been necessary. Expected are increasing recovery rates with increasing height. Additionally, an analysis of the plume shape via a drone or a mobile high resolution measurement device could give qualitative information on concentration profile at the release from the building and would add to a better interpretation of the IDM emission data.

Thus, with using the bLS model and the IDM, it is more likely to underestimate emissions than overestimating them. However, it is not possible to conclude from the present study how many times underestimation of housing emissions determined with a bLS model occur, as there were studies showing good results with the bLS model in comparable situations (Bühler et al., 2021; Gao et al., 2010).

## 5 Conclusions

The median recovery rates of the release experiment were 0.56 - 0.71 and thus, smaller than 1, which cannot be conclusively explained. We hypothesise that the barn and the tree in the main wind axis have led to the systematic underestimation of the IDM-derived emission rates due to the deviations of the wind field and turbulent dispersion from the ideal assumptions in the bLS model. However, information regarding the shape of the plume was not available. It is important to note that the present study does not provide conclusive evidence that the IDM generally underestimates barn emissions. Other IDM studies have shown near 100% recovery for similar release experiments or good agreement with with an independent reference method. However, more experiments, where the target gas is released inside a barn, or a tracer ratio method is used as validation, might

https://doi.org/10.5194/amt-2023-258
Preprint. Discussion started: 5 February 2024


Atmospheric Measurement Techniques Discussions

be needed to better understand the limitations of the IDM. Our recommendations for barn measurements with IDM are that despite following all recommendations, there is no 100% guarantee that the IDM will provide accurate emission results. Therefore, we recommend that experiments be carried out carefully and one should be aware that deviations might occur. Downwind profile measurements of the concentration or a qualitative plume mapping with a drone or a mobile high resolution measurement device might help to see if such deviations occur.

**Author contributions**

TK was responsible for funding acquisition; MB, CH and TK were for responsible for conceptualisation; MB and PB were responsible for conducting the $CH_4$ release; MB and CH were responsible for data evaluation; MB was responsible for the visualisation; MB was responsible for writing the original draft with inputs from CH, AN, CA and TK.

**Competing interests**

At least one of the co-authors is a member of the editorial board of Atmospheric Measurement Techniques.

**Data**

The treated data of the MC and IC2 can be found in the supporting information.

**Acknowledgements**

Funding from the Swiss Federal Office for the Environment (Contract number: 00.5082.PZ/BECDD68E6) is gratefully acknowledged. We thank the owner of the barn and farmers of the land in the surrounding areas for their collaboration and assistance. We thank Simon Bowald for the planning of the $CH_4$ source and Simon Bowald and Martin Häberli-Wyss for their support during the measurements (both School of Agricultural, Forest and Food Sciences, Zollikofen).

**References**

Baldé, H., VanderZaag, A. C., Burtt, S., Evans, L., Wagner-Riddle, C., Desjardins, R. L., and MacDonald, J. D.: Measured versus modeled methane emissions from separated liquid dairy manure show large model underestimates, Agriculture, Ecosystems & Environment, 230, 261-270, 10.1016/j.agee.2016.06.016, 2016a.

Baldé, H., VanderZaag, A. C., Burtt, S. D., Wagner-Riddle, C., Crolla, A., Desjardins, R. L., and MacDonald, D. J.: Methane emissions from digestate at an agricultural biogas plant, Bioresour Technol, 216, 914-922, 10.1016/j.biortech.2016.06.031, 2016b.

https://doi.org/10.5194/amt-2023-258
Preprint. Discussion started: 5 February 2024




Bühler, M., Häni, C., Ammann, C., Mohn, J., Neftel, A., Schrade, S., Zähner, M., Zeyer, K., Brönnimann, S., and Kupper, T.: Assessment of the inverse dispersion method for the determination of methane emissions from a dairy housing, Agricultural and Forest Meteorology, 307, 108501, 10.1016/j.agrformet.2021.108501, 2021.

Bühler, M., Häni, C., Ammann, C., Brönnimann, S., and Kupper, T.: Using the inverse dispersion method to determine methane emissions from biogas plants and wastewater treatment plants with complex source configurations, Atmospheric Environment: X, 13, 100161, 10.1016/j.aeaoa.2022.100161, 2022.

Flesch, T. K., Wilson, J. D., and Yee, E.: Backward-time Lagrangian stochastic dispersion models and their application to estimate gaseous emissions, Journal of Applied Meteorology, 34, 1320-1332, Doi 10.1175/1520-0450(1995)034<1320:Btlsdm>2.0.Co;2, 1995.

Flesch, T. K., Wilson, J. D., Harper, L. A., Crenna, B. P., and Sharpe, R. R.: Deducing ground-to-air emissions from observed trace gas concentrations: A field trial, Journal of Applied Meteorology, 43, 487-502, Doi 10.1175/1520-0450(2004)043<0487:Dgefot>2.0.Co;2, 2004.

Flesch, T. K., Wilson, J. D., Harper, L. A., and Crenna, B. P.: Estimating gas emissions from a farm with an inverse-dispersion technique, Atmospheric Environment, 39, 4863-4874, 10.1016/j.atmosenv.2005.04.032, 2005.

Flesch, T. K., Harper, L. A., Powell, J. A., and Wilson, J. D.: Inverse-dispersion calculation of ammonia emissions from Wisconsin dairy farms, Transactions of the Asabe, 52, 253-265, 10.13031/2013.25946, 2009.

Flesch, T. K., Verge, X. P. C., Desjardins, R. L., and Worth, D.: Methane emissions from a swine manure tank in western Canada, Canadian Journal of Animal Science, 93, 159-169, 10.4141/Cjas2012-072, 2013.

Gao, Z. L., Desjardins, R. L., and Flesch, T. K.: Assessment of the uncertainty of using an inverse-dispersion technique to measure methane emissions from animals in a barn and in a small pen, Atmospheric Environment, 44, 3128-3134, 10.1016/j.atmosenv.2010.05.032, 2010.

Gerber, P. J.: Tackling climate change through livestock: A global assessment of emissions and mitigation opportunities, Food and Agriculture Organization of the United Nations FAO, Rome2013.

Häni, C., Flechard, C., Neftel, A., Sintermann, J., and Kupper, T.: Accounting for field-scale dry deposition in backward Lagrangian stochastic dispersion modelling of NH3 emissions, Atmosphere, 9, 146, 10.3390/atmos9040146, 2018.

Hrad, M., Vesenmaier, A., Flandorfer, C., Piringer, M., Stenzel, S., and Huber-Humer, M.: Comparison of forward and backward Lagrangian transport modelling to determine methane emissions from anaerobic digestion facilities, Atmospheric Environment-X, 12, 100131, ARTN 100131 10.1016/j.aeaoa.2021.100131, 2021.

Laubach, J., Bai, M., Pinares-Patino, C. S., Phillips, F. A., Naylor, T. A., Molano, G., Rocha, E. A. C., and Griffith, D. W. T.: Accuracy of micrometeorological techniques for detecting a change in methane emissions from a herd of cattle, Agricultural and Forest Meteorology, 176, 50-63, 10.1016/j.agrformet.2013.03.006, 2013.

McGinn, S. M., Flesch, T. K., Harper, L. A., and Beauchemin, K. A.: An approach for measuring methane emissions from whole farms, J Environ Qual, 35, 14-20, 10.2134/jeq2005.0250, 2006.

Sommer, S. G., Christensen, M. L., Schmidt, T., and Jensen, L. S.: Animal manure recycling, John Wiley & Sons, Ltd, Chichester, UK, 10.1002/9781118676677, 2013.

Stocker, T. F., Qin, D., Plattner, G.-K., Alexander, L. V., Allen, S. K., Bindoff, N. L., F.-M., B., Church, J. A., Cubasch, U., Emori, S., Forster, P., P., F., Gillett, N., Gregory, J. M., Hartmann, D. L., Jansen, E., Kirtman, B., Knutti, R., Krishna Kumar, K., Lemke, P., Marotzke, J., Masson-Delmotte, V., Meehl, G. A., Mokhov, I. I., Piao, S., Ramaswamy, V., Randall, D., Rhein, M., Rojas, M., Sabine, C., Shindell, D., Talley, L. D., Vaughan, D. G., and Xie, S.-P.: Technical Summary: In: Climate Change 2013: The Physical Science Basis. Contribution of Working Group I to the Fifth Assessment Report of the Intergovernmental Panel on Climate Change, 2013.

VanderZaag, A. C., Gordon, R. J., Glass, V. M., and Jamieson, R. C.: Floating covers to reduce gas emissions from liquid manure storages: A review, Applied Engineering in Agriculture, 24, 657-671, 10.13031/2013.25273, 2008.